

Supporting Information

High-Performance Transparent Conductive Pyrolyzed Carbon (Py-C) Ultrathin Film

Monalisa Pal,^{a†} Gilwoon Lee,^{a†} Anupam Giri,^a Kaliannan Thiyagarajan,^a Kangkyun Baek,^b Manish Kumar,^c and Unyong Jeong^{a*}

^a *Department of Materials Science and Engineering, Pohang University of Science and Technology, 77 Cheongam-Ro, Nam-Gu, Pohang 37673, Korea.*

^b *Center for Self-assembly and Complexity, Institute for Basic Science, Pohang 37673, Republic of Korea.*

^c *Pohang Accelerator Laboratory (PAL), Pohang University of Science and Technology, 77 Cheongam-Ro, Nam-Gu, Pohang 790-784, Korea.*

† Those authors equally contributed to this work.

[*] Corresponding author: E-mail: ujeong@postech.ac.kr

Table S1. Other graphitic thin films synthesized by various processes.

	Journal	Title	Synthesis process	Sheet resistance	Transmittance (%) at 550 nm	Reference
1	Small 2011, 7, 3186–3192.	Flexible and Transparent Electrothermal Film Heaters Based on Graphene Materials.	Thermal annealing (at 800, 900, 1000 °C)	6,079 1,568 0.641	81 53 34	[24]
2	Appl. Surf. Sci. 2018, 435, 809–814	Large-Area Self-Assembled Reduced Graphene Oxide/Electrochemically Exfoliated Graphene Hybrid Films for Transparent Electrothermal Heaters.	GO/EEG-HI thermal annealing at 800 °C EEG=electrochemically exfoliated graphene	89.8 48.9 5.3 3	81.4 76.5 79.7 76.2	[25]
3	Thin Solid Films 2014, 556, 13–17.	Flexible, Transparent, and Conductive Defrosting Glass.	Chemical reduction with hydrazine hydrate at 800 °C	2 5.37 10	24.9– 45 68.4	[26]
4	Adv. Funct. Mater. 2009, 19, 2577–2583.	Evolution of Electrical, Chemical, and Structural Properties of Transparent and Conducting Chemically Derived Graphene Thin Films.	Ar/H ₂ annealing at 1100 °C	372–743312	46.2–96.2	[27]
5	Nano Lett. 2008, 8, 323–327.	Transparent, Conductive Graphene Electrodes for Dye-Sensitized Solar Cells.	Ar/H ₂ annealing at 1100 °C	1800	60	[28]
6a	ACS Nano 2008, 2, 463–470.	Evaluation of Solution-Processed Reduced Graphene Oxide Films as Transparent Conductors.	N ₂ H ₄ + thermal annealing at 400 °C	50000	80	[29]
6b			Thermal annealing at 1100 °C	5000	80	[29]
7	Nat. Nanotechnol. 2008, 3, 101–105.	Processable Aqueous Dispersions of Graphene Nanosheets.	N ₂ H ₂ reduction in solution	~20000000	96	[30]
8	Nat. Nanotechnol. 2008, 3, 538–542	Highly Conducting Graphene Sheets and Langmuir–Blodgett Films.	Langmuir–Blodgett film calcined at 350 °C	8000–150000	79–92	[31]
9	Nano Lett. 2015, 15, 5846–5854	Direct Chemical Vapor Deposition-Derived Graphene Glasses Targeting Wide Ranged Applications	atmospheric-pressure CVD	1700–6100	57–92	[32]
10	Nat. Nanotechnol. 5, 574–578 (2010).	Roll-to-roll production of 30-inch graphene films for transparent electrodes.	CVD over Cu foil	275	97.4	[14]
11	Nature 457, 706–710 (2009)	Large-scale pattern growth of graphene films for stretchable transparent electrodes.	CVD over Ni	290–700	76.3–83.7	[33]
12	Science Advances 2016, 2	Ultra-smooth glassy graphene thin films for flexible transparent circuits.	PEI+Glucose spin coat over quartz, Annealing 1000°C, ramping 2°C/min, reannealing using Ni, at 850 °C.	1000	89	[5]
13	Nanoscale Res Lett 2016, 11, 54–54.	Ultra-thin Graphitic Film: Synthesis and Physical Properties.	CVD on Cu foil at 1000 °C	1150	75	[9]
14	Applied Surface Science 256 (2010) 6186–6190	Transparent ultrathin conducting carbon films	Thermal annealing of negative PR AZ nLOF 2070 at 1000°C	11000	80	[18]

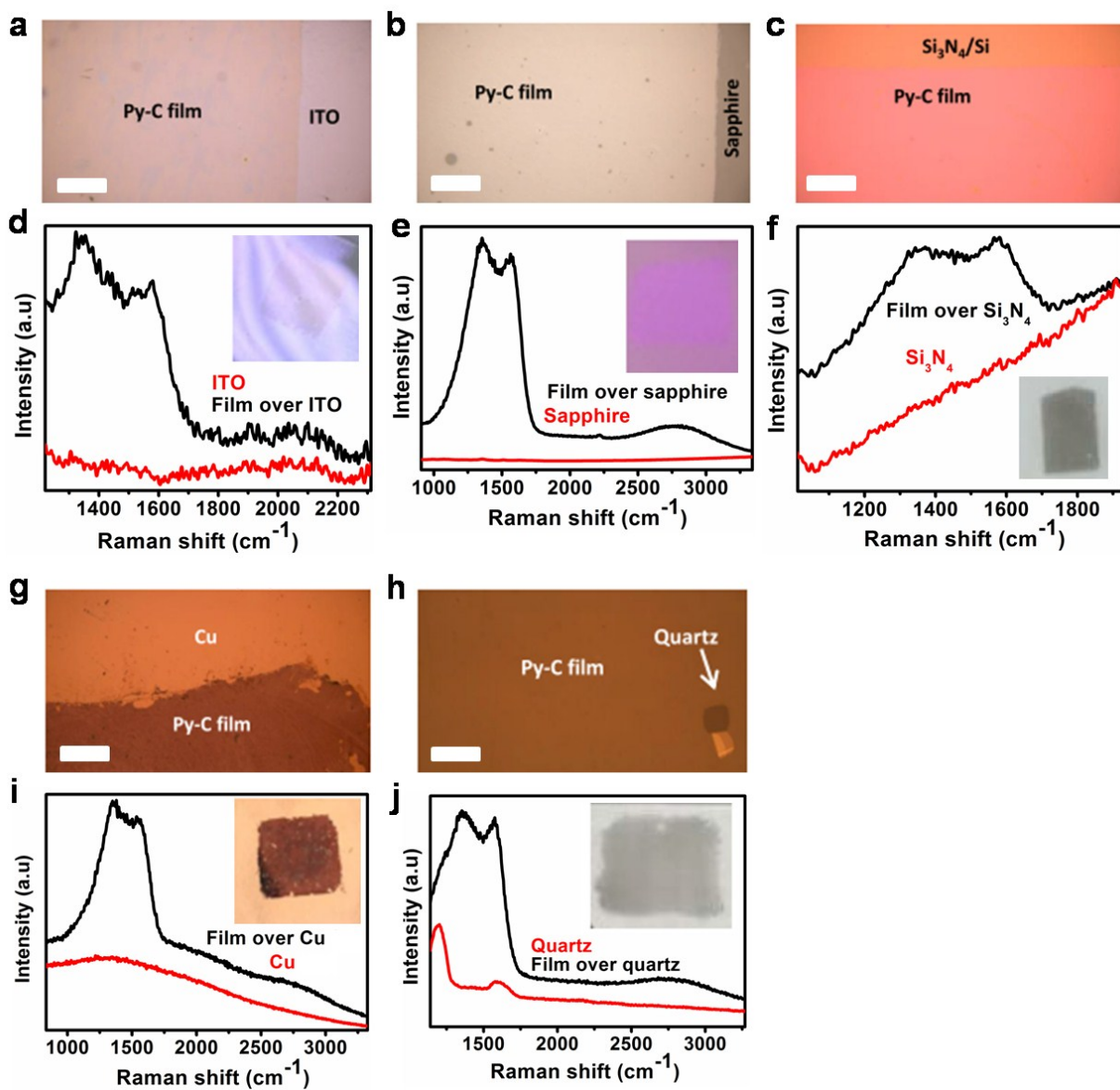


Figure S1: (a), (b), (c), (g), and, (h) OM image, (d), (e), (f), (i), and, (j) Raman spectra of Py-C film grown over ITO, sapphire, Si₃N₄ /Si, Cu, and quartz. Scale bar in OM images is 500 μm . Inset shows the camera images of the Py-C film grown over each substrate.

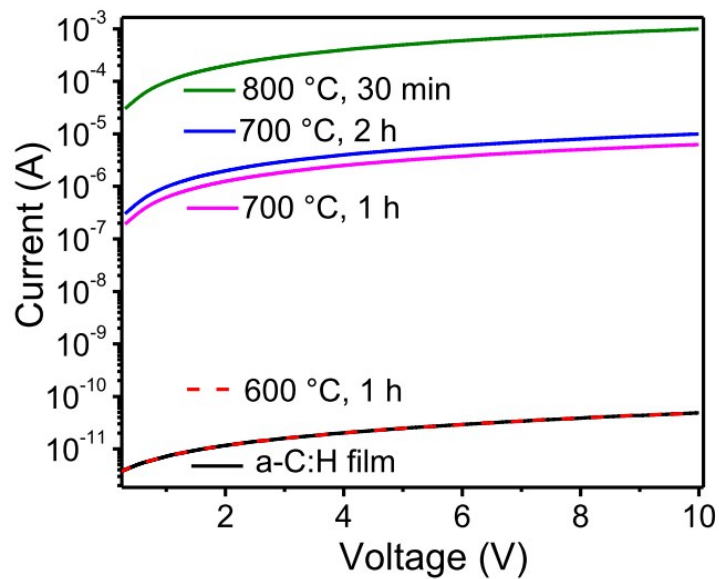


Figure S2: Optimization of annealing temperature and time for the conversion of a-C:H film to Py-C film.

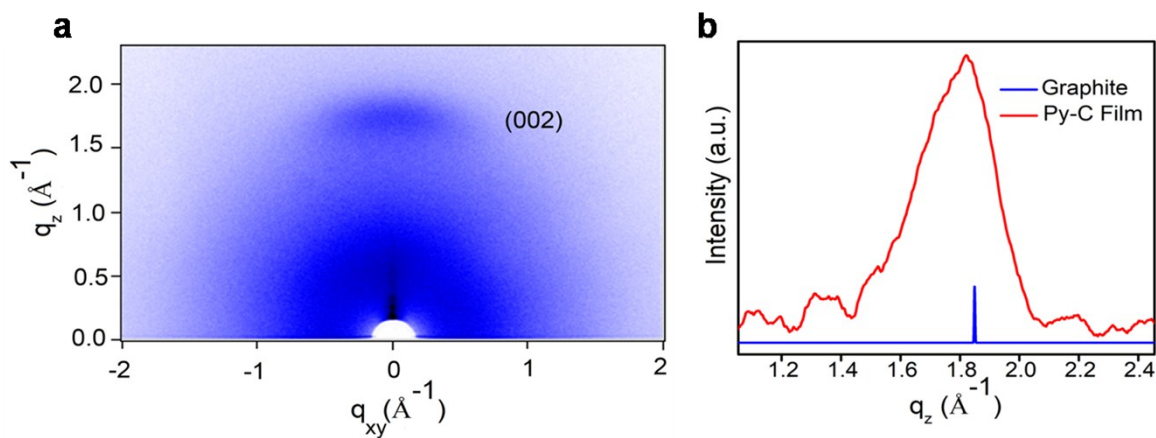


Figure S3: (a) Two-dimensional grazing-incident X-ray diffraction (GIXRD) image of Py-C film. (b) Comparative one-dimensional XRD pattern of Py-C film and graphite.

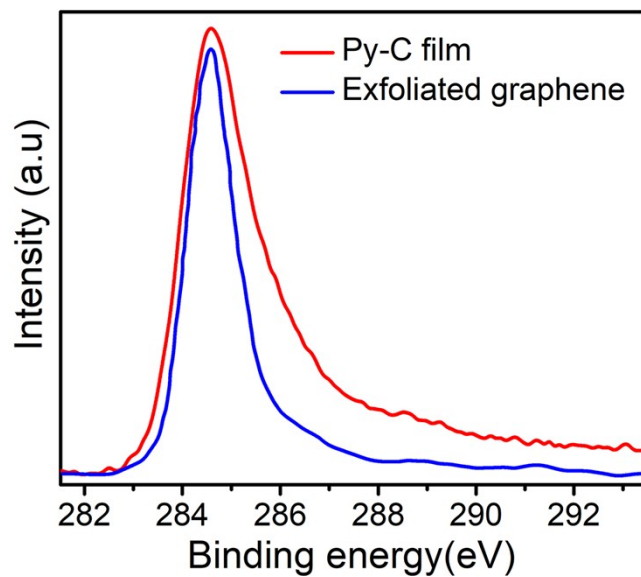


Figure S4: Comparative C1s XPS spectrum of the Py-C film and exfoliated graphene..

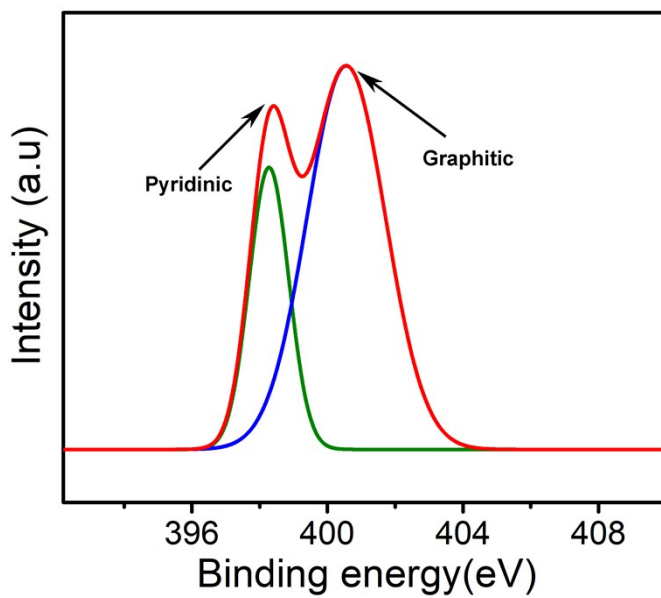


Figure S5: N1s XPS spectrum of Py-C film.

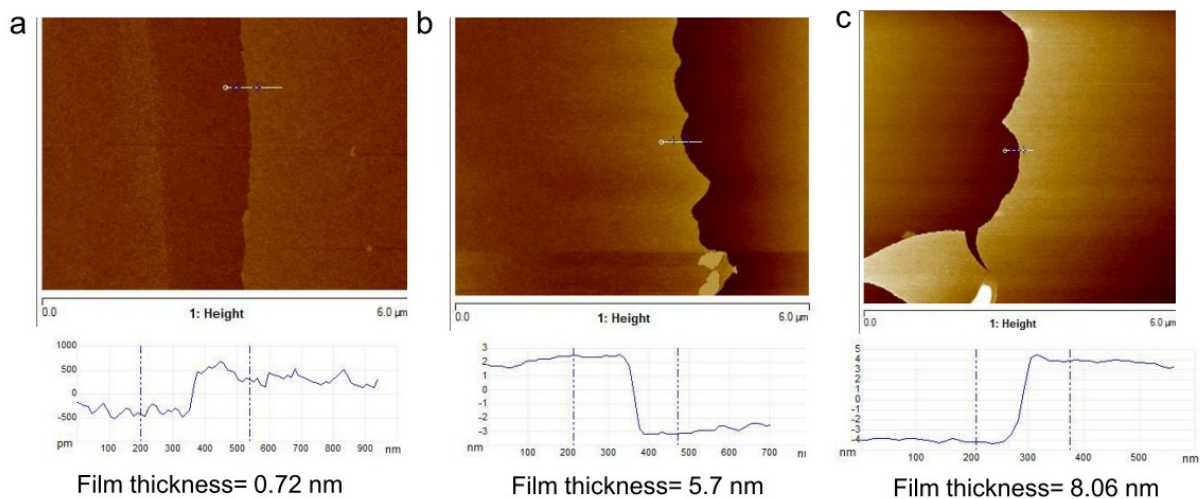


Figure S6: AFM images of Py-C films of different thickness.

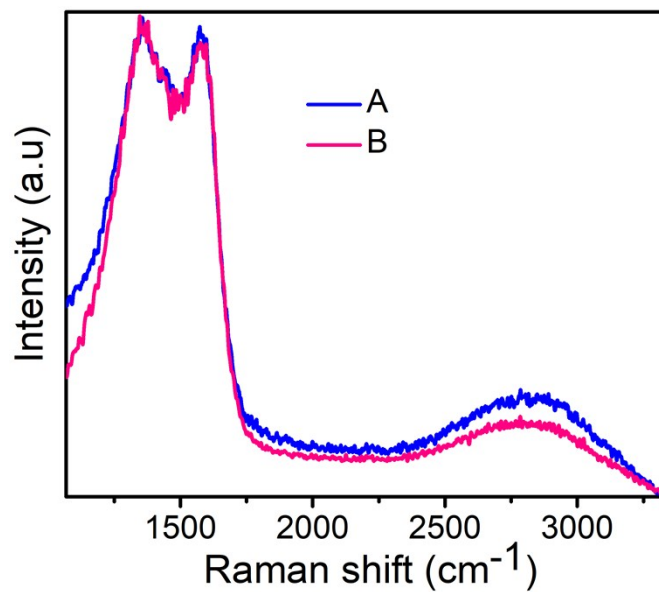


Figure S7: Raman spectra obtained from film over SiO_2/Si (A) and suspended film (B)..

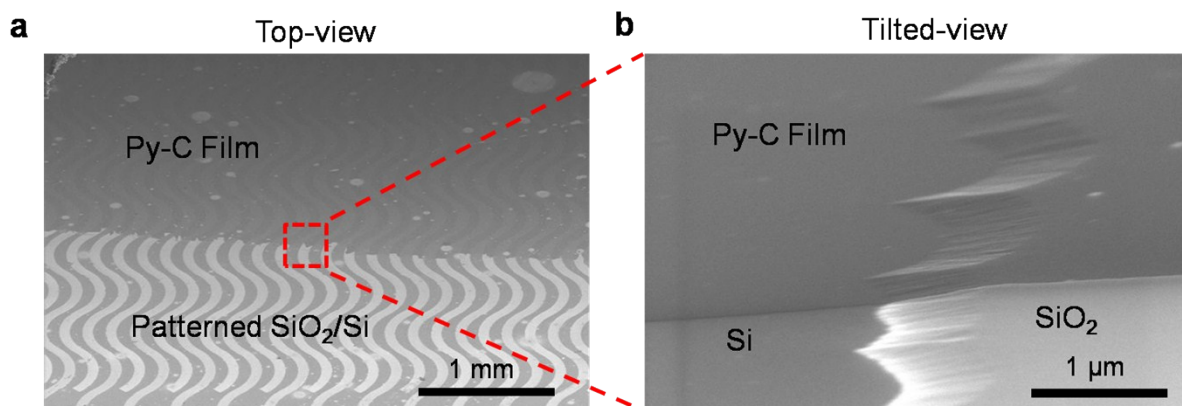


Figure S8: (a) Top-view SEM image of Py-C film grown over patterned SiO₂/Si wafer with trench width 100 μm and height 100 nm. (b) High resolution tilted-view SEM image of the marked area in (a), indicated by red box.

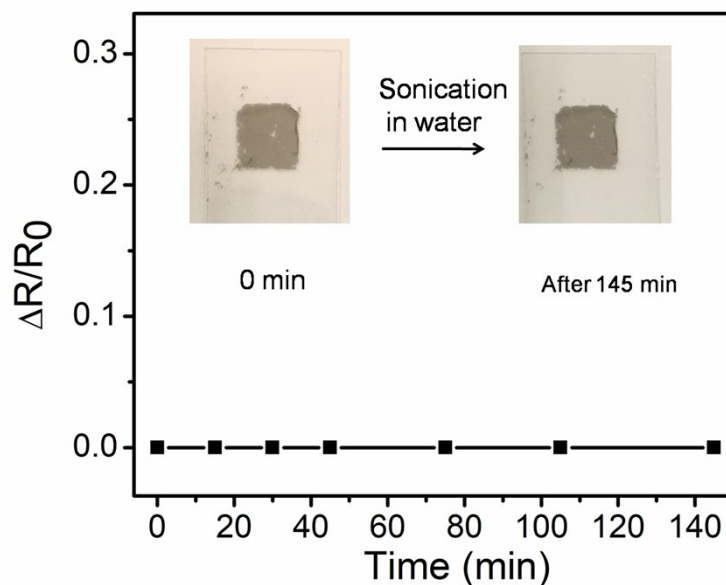


Figure S9: Adhesion test between Py-C film and the flexible substrate PET by ultrasonication in water for 145 min. Inset shows the camera image of Py-C film over PET before and after ultrasonication for 145 min.

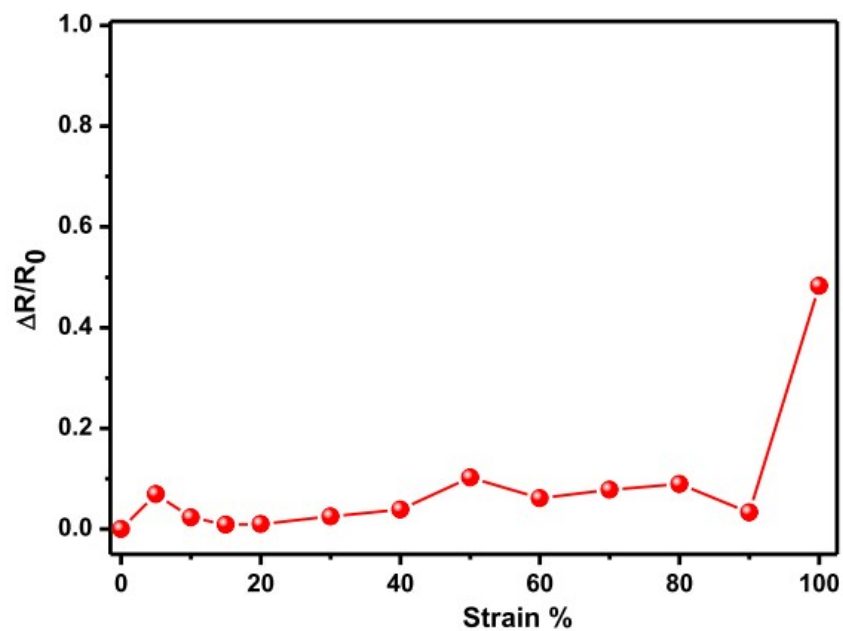


Figure S10: Change of resistance of stretchable Py-C thin film electrode with different strain.



Figure S11: 6 × 6 pixelated ACEL device at off state.

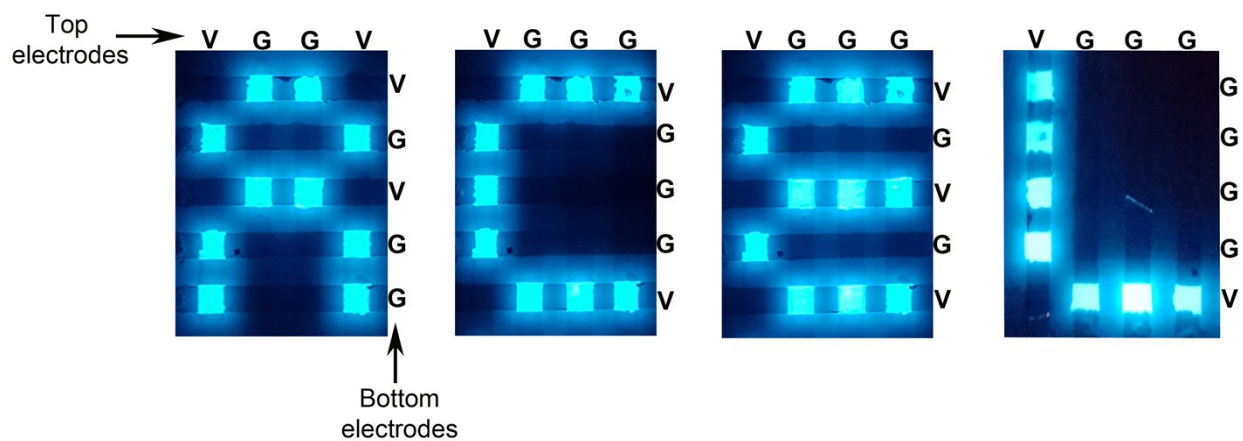


Figure S12: Principle of writing different letters in pixelated ACEL device.

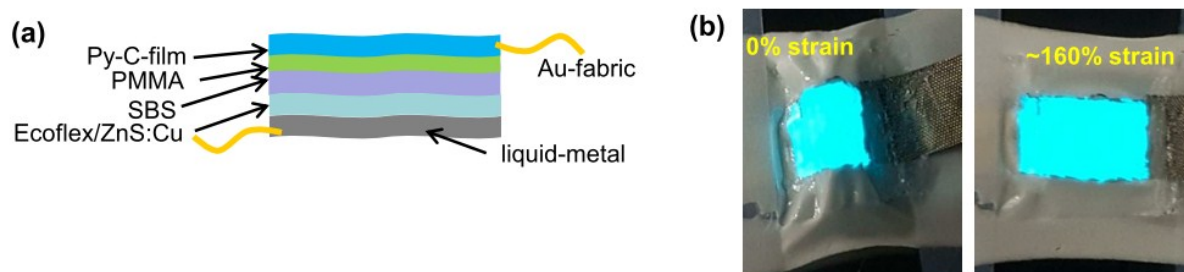


Figure S13: (a) Scheme of stretchable ACEL device made of Py-C thin film electrode on prestrained elastomer. (b) Photograph of stretchable ACEL device before (left) and after 160% stretching (right).